Journal of Catalysis 266 (2009) 369–379

Contents lists available at ScienceDirect

Journal of Catalysis

journal homepage: www.elsevier.com/locate/jcat

Preparation of high-performance MoP hydrodesulfurization catalysts via a sulfidation–reduction procedure

Yang Teng [a], Anjie Wang [a,b,*], Xiang Li [a,b], Jianguo Xie [a], Yao Wang [b], Yongkang Hu [a,b]

[a] State Key Laboratory of Fine Chemicals, School of Chemical Engineering, Dalian University of Technology, Dalian 116012, PR China
[b] Liaoning Key Laboratory of Petrochemical Technology and Equipments, Dalian University of Technology, Dalian 116012, PR China

ARTICLE INFO

Article history:
Received 10 May 2009
Revised 2 July 2009
Accepted 8 July 2009
Available online 7 August 2009

Keywords:
Molybdenum phosphide
Preparation
Sulfidation
Hydrodesulfurization
Dibenzothiophene
4,6-Dimethyldibenzothiophene

ABSTRACT

MoP/MCM-41 was prepared from its oxidic precursors by sulfidation at 400 °C for 3 h using 10% H_2S/H_2, followed by temperature-programed reduction in H_2. The resulting catalyst, MoP/MCM-41(SR), showed considerably a higher catalytic activity in the hydrodesulfurization (HDS) of dibenzothiophene (DBT) and 4,6-dimethyldibenzothiophene (4,6-DMDBT) than a catalyst prepared by temperature-programed reduction (MoP/MCM-41(R)). 4,6-DMDBT exhibited much higher activity than DBT both in independent and in simultaneous HDS. Comparison of the HDS performance of MoP/MCM-41(SR) with mixtures of MoP/MCM-41(R) and MoS_2/MCM-41 excluded the synergetic effect of separate MoS_2 and MoP phases in MoP/MCM-41(SR). XRD characterization indicated that smaller molybdenum phosphide crystals were generated in MoP/MCM-41(SR). A shift of the Mo $3d_{5/2}$ binding energy from 228.6 to 229.1 eV was observed in the XPS spectra, which might be related with the incorporation of sulfur in the MoP structure. Moreover, the sulfidation step facilitated the formation of MoP crystals and lowered the threshold reduction temperature.

1. Introduction

Due to the increasingly stringent worldwide regulations of sulfur contents in motor fuels, deep hydrodesulfurization (HDS) has attracted great attention. One of the cost-effective approaches to deep HDS is the development of high performance HDS catalysts with new active species other than the conventional transition-metal sulfides. Metal carbides, nitrides, and phosphides all show very high activity in both HDS and hydrodenitrogenation (HDN), but carbides and nitrides are unstable in the presence of H_2S [1,2]. The deactivation is caused by the transformation of metal carbides and nitrides to sulfides under typical HDS conditions. In contrast to carbides and nitrides, metal phosphides are stable against H_2S [3,4].

Although there are several methods to synthesize metal phosphides [5–8], supported metal phosphides are generally prepared from their oxidic precursors by high-temperature reduction in H_2 [5] or by phosphidation in PH_3 [7–9]. Due to the high toxicity of PH_3, the temperature-programed H_2 reduction method is commonly used to prepare the supported metal phosphides in the field of hydrotreating catalysis.

Shu and Oyama reported that the sulfur contents of MoP and WP catalysts increased remarkably after HDS reactions [10]. Based on characterization results, Oyama et al. proposed that a phosphosulfide might form during HDS [11,12]. Prins and coworkers investigated the effect of H_2S on the HDN of *o*-propylaniline catalyzed by MoP/SiO_2 [13,14]. They found that the HDN activity decreased slightly when H_2S was added, whereas after the removal of H_2S, the activity was higher than before the addition of H_2S. Sawhill et al. [15] found that an O_2-passivated Ni_2P/SiO_2 catalyst showed a higher HDS activity when it was subjected to sulfidation by H_2S/H_2 than to H_2 reduction. Sun et al. observed the incorporation of sulfur species in a MoP catalyst after HDS [16]. It seems that sulfur atoms are involved in the active metal phosphide structure.

In this paper, we report a new procedure for the preparation of siliceous MCM-41-supported MoP from its oxidic precursors. A sulfidation step at 400 °C for 3 h with H_2S/H_2 was included in the temperature-programed reduction. The prepared MoP/MCM-41 catalysts were tested in the HDS of dibenzothiophene (DBT) and 4,6-dimethyldibenzothiophene (4,6-DMDBT), and were characterized by means of XRD, XRF, and XPS.

2. Experimental

2.1. Catalyst preparation and HDS reaction

Siliceous MCM-41 was synthesized using sodium silicate hydrate as the SiO_2 source and cetyltrimethylammonium bromide

* Corresponding author. Address: State Key Laboratory of Fine Chemicals, School of Chemical Engineering, Dalian University of Technology, Dalian 116012, PR China. Fax: +86 411 39893693.
E-mail addresses: ajwang@dlut.edu.cn, anjwang@chem.dlut.edu.cn (A. Wang).

0021-9517/$ - see front matter © 2009 Elsevier Inc. All rights reserved.
doi:10.1016/j.jcat.2009.07.003

as the template, according to a procedure reported before [17]. MoP/MCM-41 oxidic precursors were prepared by the pore volume impregnation method. In a typical preparation procedure, 3.6 g $(NH_4)_6Mo_7O_{24}{\cdot}4H_2O$ and 2.7 g $(NH_4)_2HPO_4$ were dissolved in 15 mL of deionized water to form a transparent solution. A sample of 3.0 g MCM-41 was wet impregnated with the above-mentioned solution. The resulting slurry was kept for 12 h at room temperature, and then dried at 120 °C overnight, followed by calcination in air at 500 °C for 3 h. In the preparation of the unsupported MoP precursor, the above-mentioned transparent solution was evaporated, and the resulting solid was dried at 120 °C overnight, followed by calcination in air at 500 °C for 3 h. Our preliminary investigation indicated that a maximum HDS activity was observed at a MoO_3 loading of 40 wt% with a P/Mo molar ratio of 1.0 in MoP/MCM-41. Therefore, a MoO_3 loading of 40 wt% and a Mo/P atomic ratio of 1.0 were chosen for all supported catalysts in the present study.

The oxidic precursor of MoP, supported or unsupported, was pelleted, crushed, and sieved to 20–40 mesh. A sample of 0.2 g oxidic precursor was charged into a trickle-bed reactor. The precursor was heated according to the following program: from room temperature to 400 °C at 10 °C min^{-1} in 10% H_2S/H_2 and kept for 3 h, then heated to 550 °C at 5 °C min^{-1} in H_2, to 650 °C at 1 °C min^{-1}, and was finally kept at 650 °C for 2 h. The flow rate of H_2S/H_2 was 30 mL min^{-1}, and that of H_2 was 150 mL min^{-1}. The supported catalyst is denoted as MoP/MCM-41(SR). For comparison, supported MoP was also prepared in a conventional *in situ* temperature-programed reduction method [18]. The oxidic precursor was heated from room temperature to 550 °C at 5 °C min^{-1} in H_2 at 150 mL min^{-1}, then to 650 °C at 1 °C min^{-1}, and finally kept at 650 °C for 2 h. The obtained catalyst is denoted as MoP/MCM-41(R).

The HDS reaction was performed in the same fixed-bed reactor after the reduction. A solution of 0.8 wt% DBT or 4,6-DMDBT in decalin was used as the feed. DBT was synthesized from biphenyl and sulfur [19], and 4,6-DMDBT and decalin were of A.R. grade. The HDS reactions of DBT and 4,6-DMDBT were conducted at 4.0 MPa. The catalytic performance was investigated either by varying reaction temperature (300–360 °C) at constant weight time (50 g min mol^{-1}) or by varying weight time (12–62 g min mol^{-1}) at 300 °C. Sampling of liquid products was started 6 h after the reaction conditions had been reached. For each run, three to five liquid samples were collected at an interval of 20 min. Both feed and products were analyzed on an Agilent-6890$^+$ gas chromatograph equipped with an FID using an HP-5 capillary column (5% phenyl methyl polysiloxane, 30.0 m × 320 μm × 0.25 μm).

In the HDS of DBT, two sulfur-containing intermediates, tetrahydrodibenzothiophene (TH-DBT) and hexahydrodibenzothiophene (HH-DBT), were detected in the products. HDS conversion is defined as follows:

$$\text{HDS conversion} = (C_{\text{DBT0}} - C_{\text{DBT}} - C_{\text{TH-DBT}} - C_{\text{HH-DBT}})/C_{\text{DBT0}} \times 100\% \quad (1)$$

where C_{DBT0} represents the DBT concentration in the feed; C_{DBT}, $C_{\text{TH-DBT}}$, and $C_{\text{HH-DBT}}$ are the concentrations of DBT, TH-DBT, and TH-DBT in the product, respectively.

Similarly, two sulfur-containing intermediates, tetrahydrodimethyldibenzothiophene (TH-DMDBT) and hexahydrodimethyldibenzothiophene (HH-DMDBT), were observed in the HDS products of 4,6-DMDBT. Decahydrodimethyldibenzothiophene (DH-DMDBT) was not detected in the products. Therefore, the HDS conversion of 4,6-DMDBT is defined as follows:

$$\text{HDS conversion} = (C_{\text{DMDBT0}} - C_{\text{DMDBT}} - C_{\text{TH-DMDBT}} - C_{\text{HH-DMDBT}})/C_{\text{DBT0}} \times 100\% \quad (2)$$

where C_{DMDBT0} represents the 4,6-DMDBT concentration in the feed, and C_{DMDBT}, C_{THDBT}, and C_{HHDBT} are the concentrations of 4,6-DMDBT, TH-DMDBT, and HH-DMDBT in the HDS product.

To check whether or not MoS_2 exists as a separate phase in MoP/MCM-41(SR), a mixture of MoS_2/MCM-41 and MoP/MCM-41(R) was tested in the HDS of DBT. MoS_2/MCM-41 was prepared by sulfidation of MoO_3/MCM-41 at 400 °C in 10% H_2S/H_2 for 3 h. The MoP/MCM-41(R) sample was passivated with 0.5 mol% O_2/Ar at room temperature.

2.2. Catalyst characterization

X-ray diffraction (XRD) patterns of the catalysts were measured on a Rigaku D/Max 2400 diffractometer using nickel-filtered Cu Kα radiation at 40 kV and 100 mA. High-resolution transmission electron microscopy (HRTEM) was performed on an FEI Tecnai G^2 F30 S-Twin electron microscope equipped with a field emission gun, working at an acceleration voltage of 300 kV. Elemental compositions were determined by means of an X-ray Fluorescence (XRF) analyzer (RSR 3400X). X-ray photoelectron spectroscopy (XPS) was performed on a Shimadzu ESCA 750 spectrometer with monochromatic Mg K exciting radiation (8 kV, 30 mA) at 5×10^{-4} Pa. Binding energies were corrected using the C (1s) peak at 284.5 eV of adventitious carbon as a reference.

Temperature-programed reduction (TPR) profiles of MCM-41-supported oxidic precursors were measured on a Chembet-3000 analyzer. Before the measurement, the sample was pretreated in He at 200 °C for 2 h. A gas mixture of 10 mol% H_2/Ar was used as the reacting agent. The TPR profiles were measured from 100 to 950 °C at 10 °C min^{-1}.

The CO uptake was measured using the pulsed chemisorption on a Chembet-3000 analyzer according to the literature [20]. A passivated sample (0.1 g), which had been exposed to air during the transfer, was re-reduced in a H_2 flow to remove the passivation layer prior to the measurement. The reactor was then cooled to 30 °C in a flow of H_2. An Ar flow (40 mL min^{-1}) was used to flush the catalyst for 30 min to achieve a clean catalyst surface. After pretreatment, 1.25 mL pulses of 1.0 mol% CO/Ar were injected into a flow of Ar (80 mL min^{-1}). CO pulses were repeatedly injected until no further CO adsorption was observed. The CO uptake of the sample was calculated from the accumulated differences in the peak areas of input and output signals.

3. Results

3.1. Preparation and characterization

Fig. 1 shows the XRD patterns of MoP/MCM-41 prepared by temperature-programed reduction (MoP/MCM-41(R)) and sulfidation–reduction (MoP/MCM-41(SR)). Diffraction peaks around 27.9°, 32.2°, 43.2°, and 57.3° were observed for both MoP/MCM-41(R) and MoP/MCM-41(SR). They are characteristic of the MoP crystal phase (PDF 24-771) and are similar to those reported by others [4]. The half widths of the peaks at 32.2° and 43.2° in the patterns of MoP/MCM-41(SR) (0.58° and 0.6°) were larger than those of MoP/MCM-41(R) (0.52° and 0.54°). According to Scherrer equation, MoP particle sizes were estimated to be 13.9 and 15.6 nm for MoP/MCM-41(SR) and MoP/MCM-41(R), respectively. It is therefore suggested that higher dispersion was obtained in MoP/MCM-41(SR).

Although the supported catalyst only showed the presence of MoP, the possibility that another sulfur-containing phase is present in low concentrations or well dispersed on the MCM-41 cannot be excluded. Thus, the transformation of oxidic precursors in the course was investigated in the preparation of bulk MoP. The XRD patterns of the oxidic precursor and after different treatments

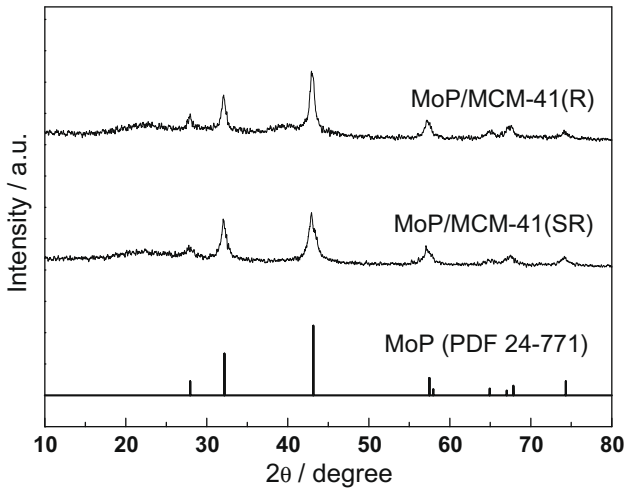

Fig. 1. XRD patterns of MCM-41-supported MoP prepared via different procedures.

are shown in Fig. 2. There were no distinct diffraction peaks in the XRD patterns of the oxidic precursor (Fig. 2a). After reduction or sulfidation at 400 °C, no diffraction peaks appeared (Fig. 2b and d). When the reduced or sulfided sample was reduced again in H_2 at 650 °C, MoP crystals were obtained, suggesting that there is a threshold temperature for the formation of MoP crystals. Nevertheless, when the oxidic precursor was treated at 650 °C in 10% H_2S/H_2 by the same procedure as temperature-programed reduction, the XRD patterns of the obtained material (Fig. 2f) showed weak characteristic diffraction peaks of the MoP phase. It is

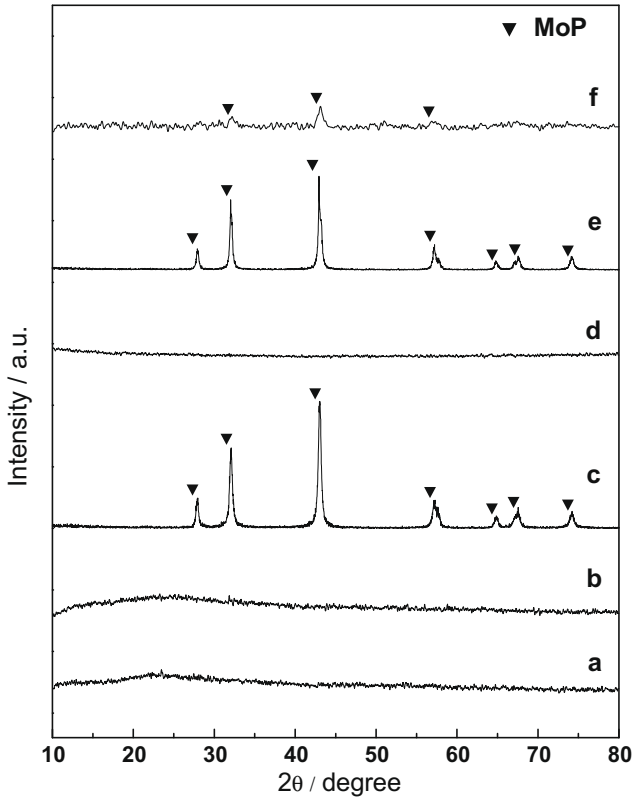

Fig. 2. XRD patterns of bulk MoP samples and the oxide precursor: (a) oxide precursor, (b) reduced at 400 °C, (c) reduced at 400 °C and then at 650 °C, (d) sulfided at 400 °C, (e) sulfided at 400 °C then reduced at 650 °C, (f) sulfided at 650 °C.

suggested that the competition of sulfidation and reduction might occur in the flow of H_2S/H_2 at 650 °C, leading to a reduction of MoP crystallinity.

Careful measurements of the bulk samples on three different X-ray diffractometers revealed that all the characteristic peaks of MoP phase shifted subtly to lower Bragg degree when the precursor was pretreated by sulfidation. For examples, the peaks of (100) and (101) crystallographic planes were 32.10° and 43.04° for the sample prepared by temperature-programed reduction, whereas 32.02° and 42.94° for that prepared by sulfidation–reduction. It is suggested that the lattice of MoP crystal increased slightly in the sample prepared by sulfidation–reduction procedure.

Fig. 3 shows the HRTEM images of bulk MoP prepared via temperature-programed reduction (a,c) and sulfidation–reduction (b,d). Both samples showed uniform and well-defined crystallites, and smaller particles were obtained in the sulfidation–reduction process, which is in agreement with XRD characterization results (22.9 and 17.4 nm, respectively). The images at high magnification (Fig. 3c and d) showed that both samples were well-ordered crystallites. A rough layer, which resulted from O_2 passivation, was observed around the MoP particles prepared by temperature-programed reduction (Fig. 3c). However, clear edges were observed in the images of the MoP particles prepared by the sulfidation–reduction procedure. The HRTEM images revealed that the lattice spacings in (100) plane of MoP crystals prepared by temperature-programed reduction and by sulfidation–reduction were averagely 0.2809 and 0.2811 nm, respectively. These observations are in agreement with the XRD characterization results (Fig. 2). It seems that sulfur might incorporate into the structure of MoP crystals, leading to a slight increase in lattice spacing.

Since the transformation of the precursors to MoP/MCM-41 is completed by temperature-programed reduction, TPR characterization may provide some insights into the reactions involved in the preparation of MoP/MCM-41. Fig. 4 illustrates the TPR profiles of MoO_3/MCM-41, MoP/MCM-41 oxidic precursor, and the sulfided MoP/MCM-41 precursor. In the profile of MoO_3/MCM-41 (Fig. 4a), two H_2 consumption peaks at 550 and 850 °C were observed. The lower temperature peak is attributed to the reduction of Mo^{6+} to Mo^{4+}, and the broad peak around 850 °C is attributed to the reduction of Mo^{4+} to Mo^0 [21]. For the MoP/MCM-41 precursor (Fig. 4b), the low temperature peak (480 °C) could be attributed to the reduction of Mo^{6+} to Mo^{4+}, whereas the high temperature peak may be assigned to the reduction of Mo^{4+} and P species to form MoP [22]. It seems that the reduction of Mo^{6+} to Mo^{4+} became easier by the addition of phosphorous to MoO_3 [23]. After the precursor had been sulfided at 400 °C, the H_2 consumption peak in the region of 480–550 °C disappeared whereas a small peak around 200 °C was observed (Fig. 4c). The peak around 200 °C may be related to the formation of H_2S from surface S species. The absence of the H_2 consumption peak in the region of 480–550 °C suggests that Mo species were transformed to Mo^{4+} or MoS_2 in sulfidation.

The XPS spectra in Mo 3d, P 2p, and S 2p regions for MoP/MCM-41(R) and MoP/MCM-41(SR) are shown in Fig. 5. All samples were passivated in a flow of a 0.5 mol% O_2/Ar, prior to exposure to air. Therefore, it is not surprising that XPS peaks corresponding to oxide species appeared in the spectra. The Mo $3d_{5/2}$ peak at 232.2 eV is associated with Mo^{6+} and Mo^{5+} species [4]. The Mo $3d_{5/2}$ peaks at 228.6 eV for MoP/MCM-41(R) and at 229.1 eV for MoP/MCM-41(SR) can be assigned to MoP species [4,20], which have a slightly higher binding energy than Mo^0 (227.4–227.8 eV) [24] but lower than Mo^{4+} (231.8 eV) [25]. The slightly higher binding energy of MoP/MCM-41(SR) than that of MoP/MCM-41(R) may be attributed to the interaction of MoP with sulfur species or the formation of phosphosulfide species. Besides the peaks corresponding to Mo^{6+} and MoP, a new XPS feature around 224.5 eV

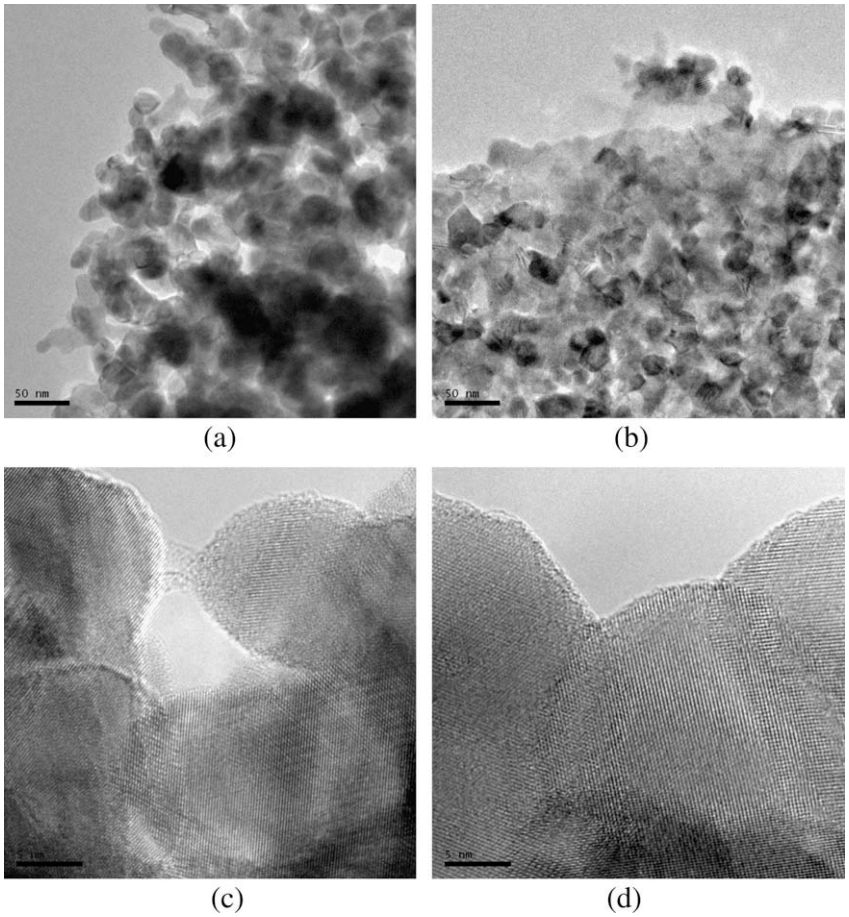

Fig. 3. HRTEM images of bulk MoP prepared by temperature-programed reduction (a,c) and by sulfidation–reduction (b,d).

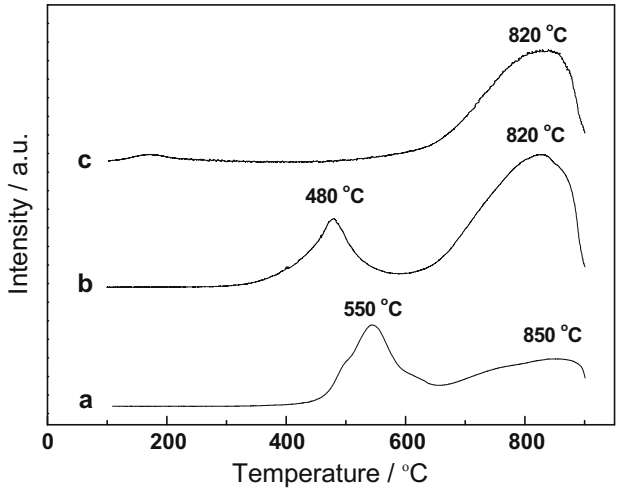

Fig. 4. TPR profiles of MoO_3/MCM-41 (a), MoP/MCM-41 oxide precursor (b), and MoP/MCM-41 oxide precursor after sulfidation (c).

characteristic of S 2s was observed in the spectrum of MoP/MCM-41(SR).

The P $2p_{3/2}$ peak at 133.9 eV in the XPS spectra of both catalysts is assigned to P^{5+} species (P_2O_5 or phosphates) [26]. These oxide species may result from the O_2 passivation. The binding energy of the P 2p peak in metal phosphides was reported to be around 129.5 eV [4]. The binding energy peak at 129.8 eV in Fig. 5b confirmed the presence of MoP in both MoP/MCM-41(SR) and MoP/MCM-41(R) catalysts. No shift of the binding energy was observed in the presence of sulfur species. A single peak at 162.4 eV was observed for MoP/MCM-41(SR) in the S 2p region (Fig. 5c). A peak in the 162.8–163.1 eV range is assigned to disulfide (S_2^{2-}), and a peak at 161.7 eV is attributed to sulfide species (S^{2-}) [27,28]. The sulfur species in MoP/MCM-41(SR) with a binding energy of 162.4 eV could be assigned to $S^{\delta-}$ species ($1 < \delta < 2$), probably corresponding to polysulfide or thiomolybdate species [29].

Table 1 summarizes the elemental compositions of MoP/MCM-41(R) and MoP/MCM-41(SR) measured by means of XRF and XPS before and after DBT HDS. It is shown that sulfur was present both in the bulk and on the surface of MoP/MCM-41(SR) particles. The surfaces of both catalysts were metal-rich relative to the bulk. After HDS, both MoP/MCM-41(SR) and MoP/MCM-41(R) gained an amount of sulfur. The atomic ratios of (P + S/2)/Mo were close to unity except for spent MoP/MCM-41(SR). The higher (P + S/2)/Mo ratio of MoP/MCM-41(SR) may be due to the presence of sulfur in the bulk of the MoP structure. Moreover, the S/Mo ratio measured by XRF was identical to that measured by XPS, indicating that sulfur was homogeneously distributed in MoP/MCM-41(SR).

3.2. HDS Performance

Fig. 6 illustrates the HDS conversion in the HDS of DBT as a function of temperature over the catalysts prepared from Mo and P oxides via different procedures. The catalyst prepared by sulfidation at 400 °C exhibited much lower HDS activity than MoP/MCM-41(SR), suggesting that the subsequent reduction in the preparation, which led to the formation of MoP phase

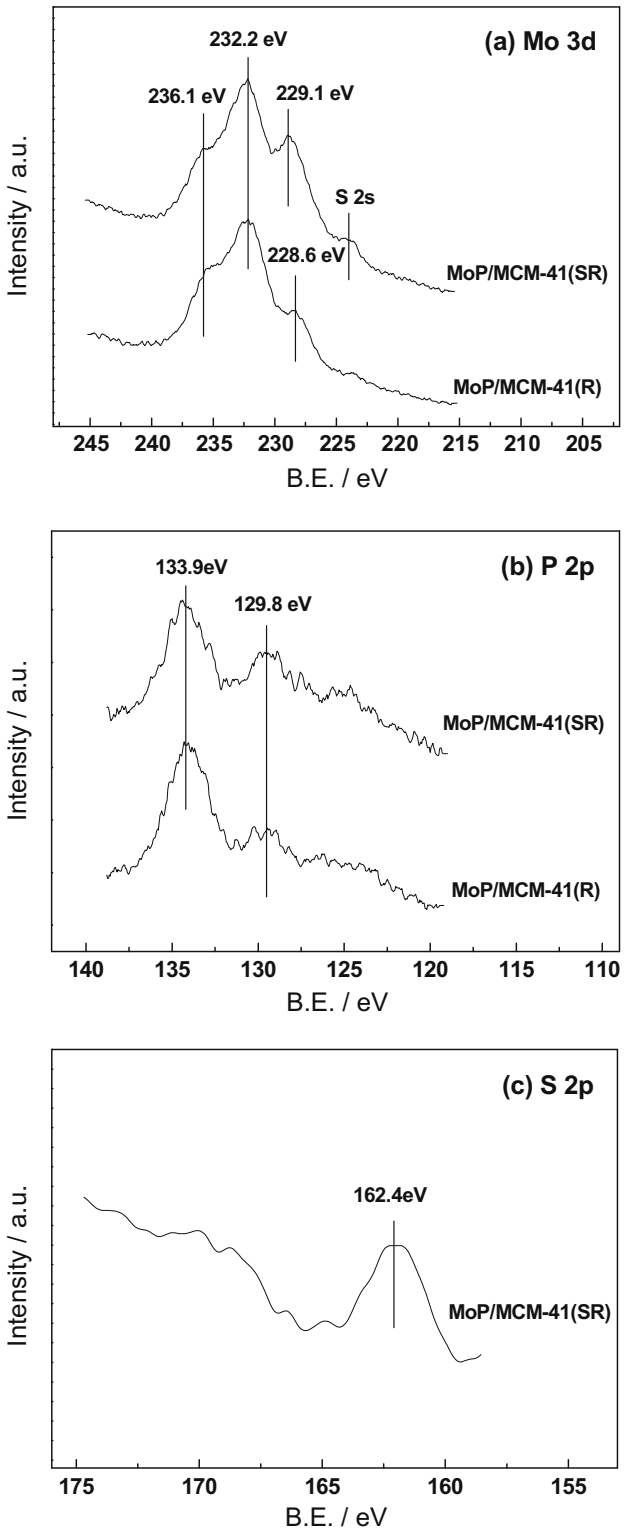

Fig. 5. XPS spectra of MoP/MCM-41 in Mo 3d (a), P 2p (b), and S 2p (c) regions.

(Fig. 2), was responsible for the enhanced HDS performance. The catalyst obtained by sulfidation at 650 °C gave only slightly higher HDS activity than the one prepared by sulfidation at 400 °C. The weak improvement in HDS activity may be related with the low crystallinity of MoP after sulfidation at 650 °C in H_2S/H_2 (Fig. 2). It is also indicated in Fig. 6 that MoP/MCM-41(SR) exhibited considerably a higher HDS activity than MoP/MCM-41(R). On the other hand, the increment in HDS conversion with temperature was smaller for MoP/MCM-41(SR) than for MoP/MCM-41(R). The higher activity and smaller increment with temperature indicate that the HDS over MoP/MCM-41(SR) had lower activation energy.

Fig. 7 shows the product selectivities in the HDS of DBT over different catalysts. The selectivity of BP, produced by the direct desulfurization pathway (DDS), was over 40% for the sulfided catalysts and MoP/MCM-41(R). Lower BP selectivity was obtained for MoP/MCM-41(SR), indicating that the other parallel pathway, hydrogenation followed by desulfurization (HYD), was enhanced. The selectivity of TH-DBT, a sulfur-containing intermediate generated from HYD pathway, was higher for the sulfided catalysts than for MoP/MCM-41(SR) and MoP/MCM-41(R). TH-DBT selectivity decreased with increasing reaction temperature for all the catalysts, indicating that high temperature favors the desulfurization of TH-DBT. With the increase in temperature, the selectivities of cyclohexylbenzene (CHB) and bicyclohexyl (BCH) hardly changed for the sulfided catalysts. The selectivity of BCH increased slightly while that of CHB decreased with increasing temperature over MoP/MCM-41(R) and MoP/MCM-41(SR). The results of both activity and selectivity suggest that sulfidation might yield different active phases than MoP.

To clarify whether or not separate MoS_2 phases are present in MoP/MCM-41(SR), we compared the HDS performance of the mixed catalysts of MoP/MCM-41(R) and MoS_2/MCM-41 with MoP/MCM-41(SR) (Fig. 8). Both mixed catalysts showed dramatically lower HDS activity than MoP/MCM-41(SR). Moreover, the product selectivities for the mixed catalysts were quite different from that for MoP/MCM-41(SR) (not shown). We therefore conclude that MoP/MCM-41(SR) was not a mixture of separate MoS_2 and MoP phases.

Fig. 9 shows the effect of final reduction temperature in the preparation on the HDS performance of MoP/MCM-41(R) and MoP/MCM-41(SR). A remarkable increase in HDS activity was observed for MoP/MCM-41(R) when the final reduction temperature was increased from 550 to 650 °C, but the improvement of the HDS activity was much lower from 450 to 550 °C. A dramatic improvement in HDS performance was observed for MoP/MCM-41(SR) when the final reduction temperature was increased from 450 to 550 °C. It is apparent that there exist threshold temperatures for both reduction procedures, and that the threshold temperature in the sulfidation–reduction procedure was lower than that in the conventional reduction method, which is in agreement with the results of XRD patterns (Fig. S1 in Supplementary material).

The conversions as a function of weight time at 300 °C in DBT HDS over MoP/MCM-41(R) and MoP/MCM-41(SR) (Fig. S2 in Supplementary material) indicated that MoP/MCM-41(SR) showed significantly higher HDS conversion at different weight time. The dependences of product selectivities on weight time are shown in Fig. 10. At short weight times, HH-DBT, in addition to TH-DBT, was detected in the HDS products for both catalysts. Higher selectivities of both TH-DBT and HH-DBT and lower BP selectivity were observed for MoP/MCM-41(SR). The selectivities of TH-DBT and HH-DBT decreased with increasing weight time for both catalysts. The selectivities of BP, CHB, and BCH did not change much with increasing weight time for DBT HDS over MoP/MCM-41(R). For MoP/MCM-41(SR), the selectivities of BP and BCH did not change considerably whereas the selectivity of BCH increased significantly with weight time. It seems that the increased BCH might originate from TH-DBT and HH-DBT, because the increase in BCH selectivity was accompanied with the decrease in the selectivities of TH-DBT and HH-DBT. The selectivity results indicated that MoP/MCM-41(SR) exhibited a higher HYD activity, which is desirable in the HDS of 4,6-DMDBT [30,31]

Consequently, we investigated the HDS of 4,6-DMDBT over MoP/MCM-41(R) and MoP/MCM-41(SR). Fig. 11 shows the

Table 1
Elemental analysis of MoP/MCM-41 catalysts determined by XRF and XPS.

Catalysts	XRF						XPS	
	Composition (wt%)			Atomic ratio			Atomic ratio	
	Mo	P	S	P/Mo	S/Mo	(P + S/2)/Mo	P/Mo	S/Mo
MoP/MCM-41(R)	25.9	7.6	0	0.96	0	0.96	0.5	0
Spent MoP/MCM-41(R)	25.3	7.2	2.0	0.88	0.24	1.00	–	–
MoP/MCM-41(SR)	26.2	7.6	1.6	0.90	0.18	0.99	0.33	0.18
Spent MoP/MCM-41(SR)	22.9	8.1	2.8	0.91	0.37	1.10	–	–

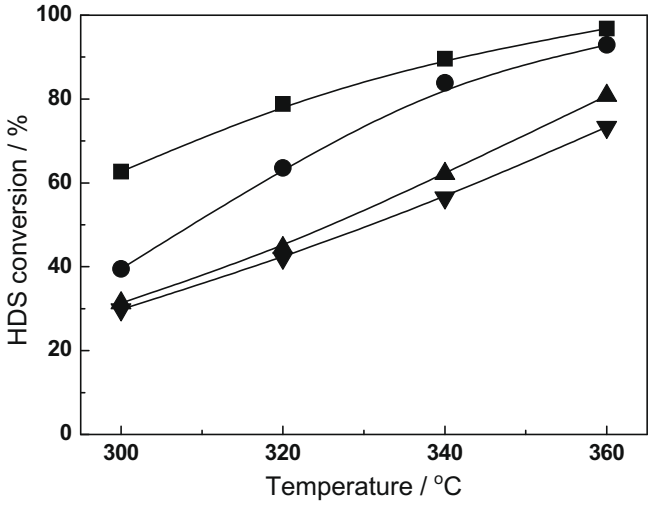

Fig. 6. HDS conversion of DBT as a function of temperature over MCM-41-supported catalysts prepared from Mo and P oxidic precursors by different procedures: (■) MoP/MCM-41(SR), (●) MoP/MCM-41(R), (▼) sulfidation at 400 °C, and (▲) sulfidation at 650 °C.

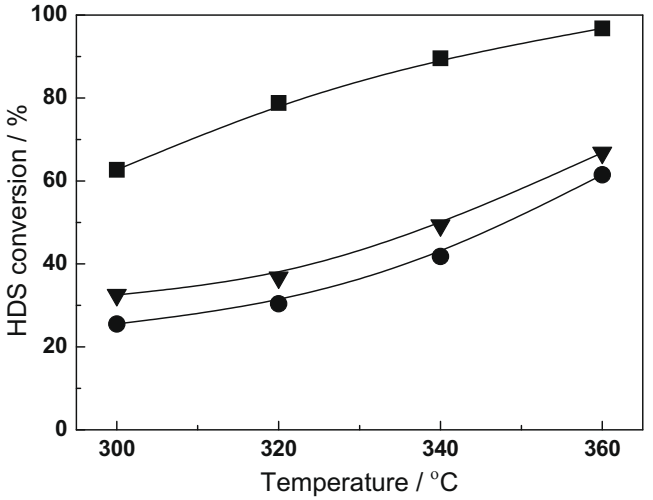

Fig. 8. HDS conversion of DBT as a function of temperature over a mixture of MoP/MCM-41 and MoS_2/MCM-41, in comparison with MoP/MCM-41(SR) (■): (▼) 90%MoP/MCM-41 + 10%MoS_2/MCM-41, (●) 80%MoP/MCM-41 + 20%MoS_2/MCM-41.

dependence of HDS conversion on temperature in the HDS of 4,6-DMDBT over both catalysts. MoP/MCM-41(SR) showed dramatically higher HDS activity than MoP/MCM-41(R) at low temperatures. The variation of product selectivities (Fig. 12) indicated that only a small amount of dimethylbiphenyl (DMBP), the product from the DDS pathway, was observed, indicating that the HYD pathway was predominant in the HDS of 4,6-DMDBT on both catalysts. However, there was a dramatic difference in the non-sulfur products generated by the HYD pathway between MoP/MCM-41(R) and MoP/MCM-41(SR). The main product was dimethylcyclohexylbenzene (DMCHB) for MoP/MCM-41(R), whereas dimethylbicyclohexyl (DMBCH) for MoP/MCM-41(SR). It seems that the HDS of 4,6-DMDBT on MoP/MCM-41(R) took place by the partial hydrogenation pathway whereas the HDS on MoP/MCM-41(SR) proceeded through the full hydrogenation pathway.

The HDS conversion of 4,6-DMDBT and product selectivities as a function of weight time at 300 °C over MoP/MCM-41(R) and

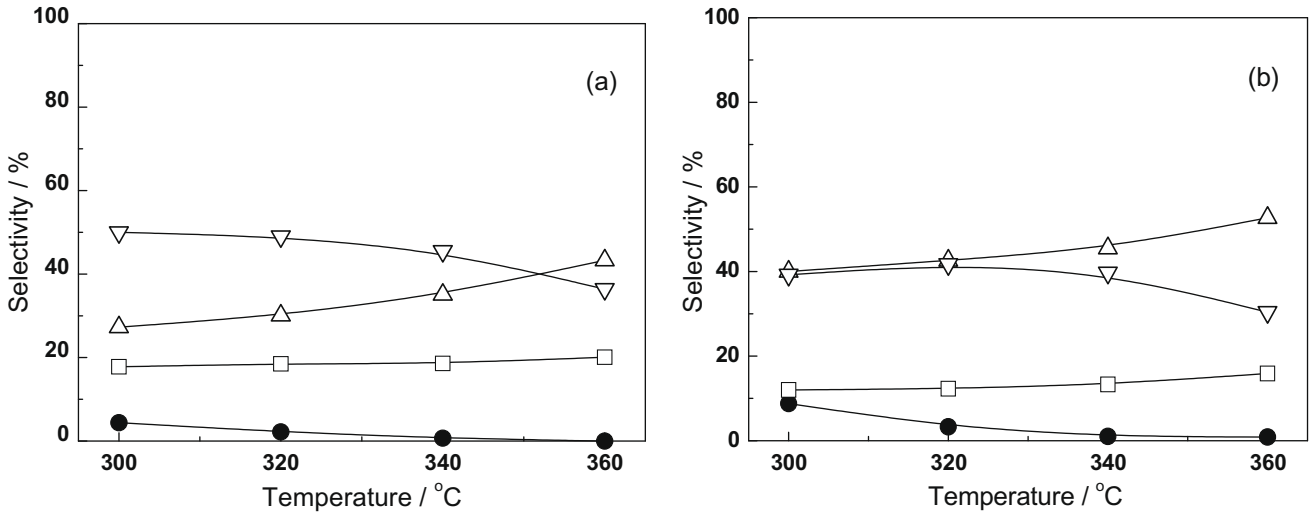

Fig. 7. Product selectivities as a function of temperature in DBT HDS over (a) MoP/MCM-41(SR), and (b) MoP/MCM-41(R); (●) TH-DBT, (△) BP, (▽) CHB, (□) BCH.

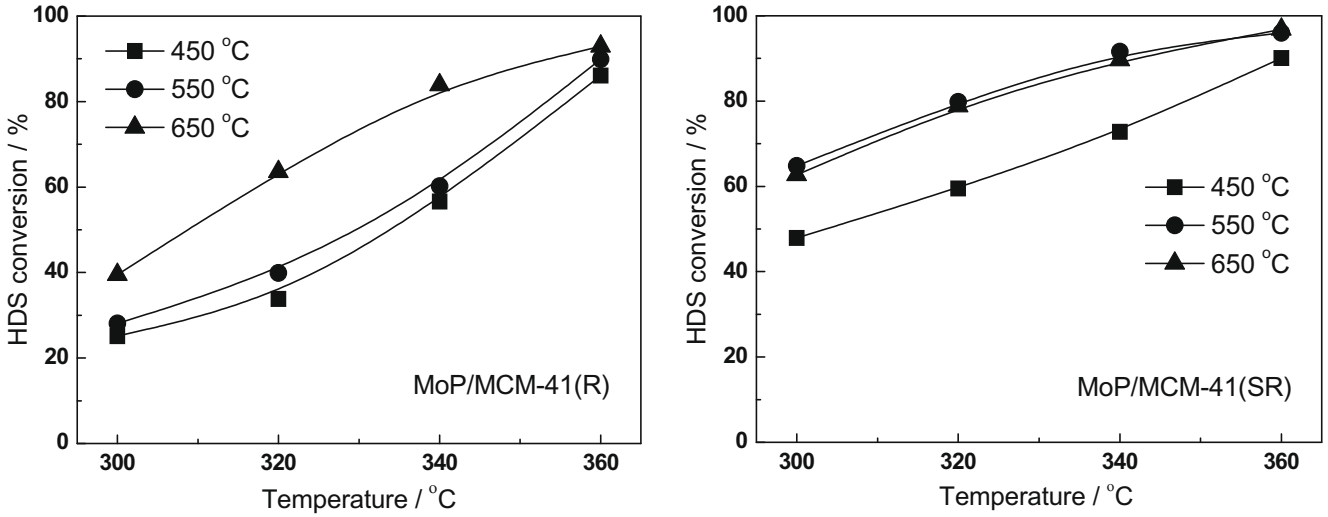

Fig. 9. HDS conversion of DBT as a function of temperature for MoP/MCM-41 catalysts prepared via different procedures at various final reduction temperatures.

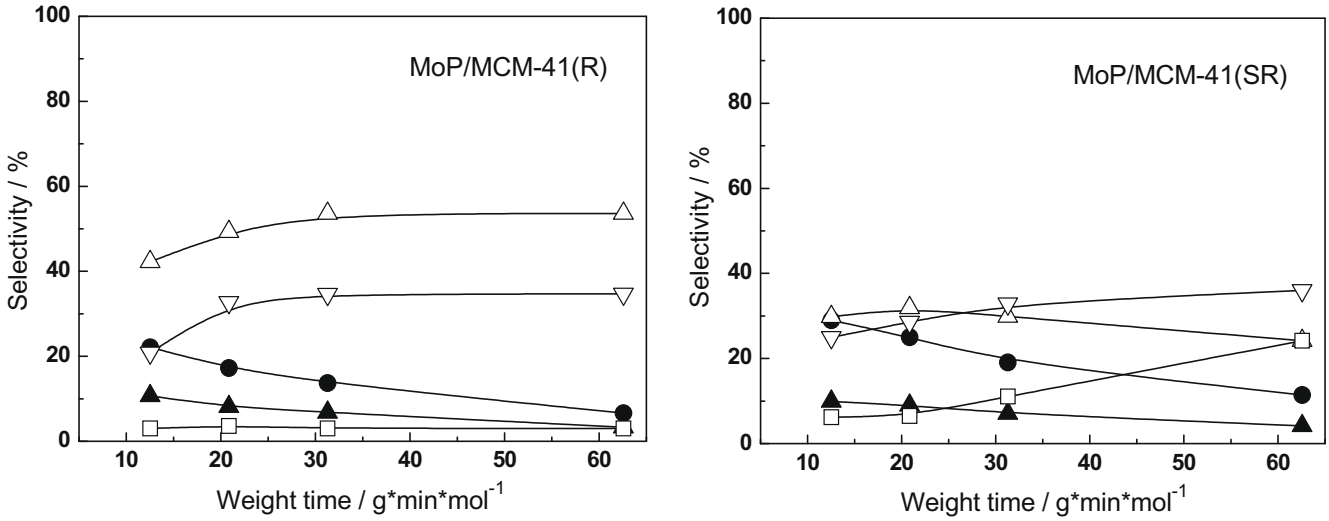

Fig. 10. Product selectivities in DBT HDS over MoP/MCM-41(R) and MoP/MCM-41(SR): (●) THDBT, (▲) HHDBT, (△) BP, (▽) CHB, (□) BCH.

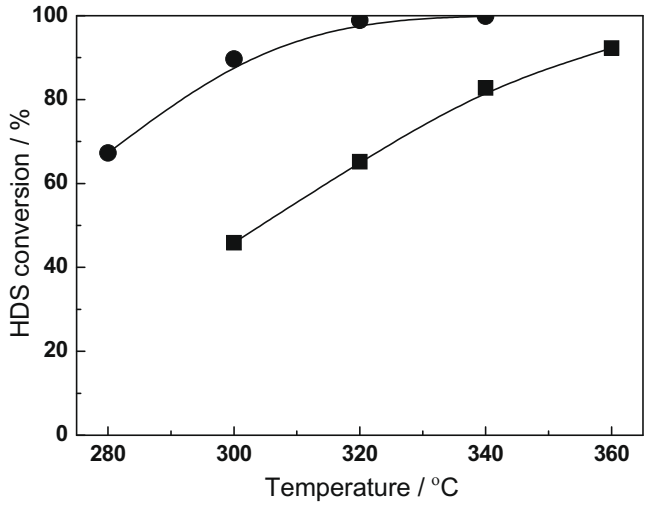

Fig. 11. HDS conversion of 4,6-DMDBT as a function of temperature for MoP/MCM-41 catalysts prepared by different procedures: (■) MoP/MCM-41(R), (●) MoP/MCM-41(SR).

MoP/MCM-41(SR) (Fig. S3 in Supplementary material) indicate that MoP/MCM-41(SR) showed much higher catalytic activity in the HDS of 4,6-DMDBT than MoP/MCM-41(R). Fig. 13 shows the variation of product selectivities at various weight times at 300 °C. In the HDS catalyzed by MoP/MCM-41(R), the selectivity of DMBP was less than 10%, and increased with weight time. The selectivity of TH-DMDBT decreased monotonously with weight time whereas that of HH-DMDBT showed a maximum around 20 g min mol^{-1}. The predominant non-sulfur product was DMCHB. The selectivities of both DMCHB and DMBCH increased with weight time, resulting from the desulfurization of both TH-DMDBT and HH-DMDBT. For MoP/MCM-41(SR), trace amount of DMBP was detected at 300 °C, and the predominant product was DMBCH. The selectivity of HH-DMDBT decreased only a little with weight time, but that of TH-DMDBT decreased dramatically at low weight time. The fast decrease of TH-DMDBT selectivity was accompanied by an increase in the selectivity of DMBCH. It is apparent that DMBCH did not form by the hydrogenation of DMCHB but from the desulfurization of TH-DMDBT.

Fig. 14 illustrates the HDS activity in the simultaneous HDS of DBT and 4,6-DMDBT on MoP/MCM-41(R) and MoP/MCM-41(SR)

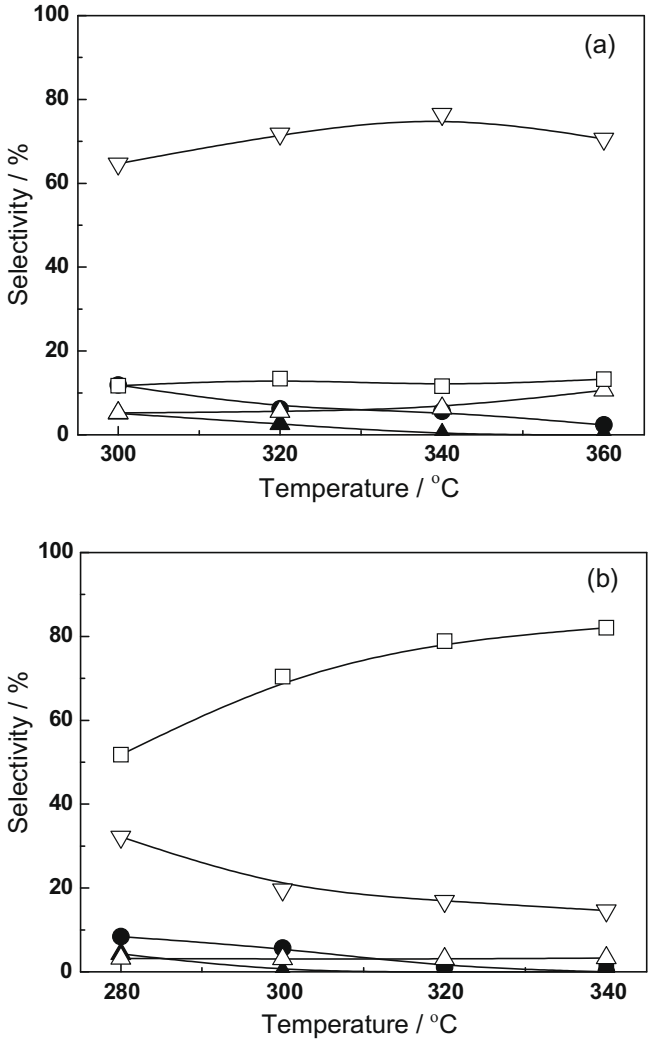

Fig. 12. Product selectivities of 4,6-DMDBT as a function of temperature for MoP/MCM-41 catalysts prepared by different procedures: (a) MoP/MCM-41(R), (b) MoP/MCM-41(SR); (●) TH-DMDBT, (▲) HH-DMDBT, (△) DMBP, (▽) DMCHB, (□) DMBCH.

at 300 °C and 4.0 MPa. A decalin solution of 0.4 wt% DBT and 0.4 wt% 4,6-DMDBT was used as the feed. It is interesting to note that 4,6-DMDBT showed a higher activity than DBT on both MoP/MCM-41(R) and MoP/MCM-41(SR) in the simultaneous HDS. The reactivity order is opposite to that for conventional sulfide catalysts, over which 4,6-DMDBT shows much lower activity than DBT.

Table 2 summarizes the catalytic performances of MoP/MCM-41(R) and MoP/MCM-41(SR) in the HDS of DBT, 4,6-DMDBT, and DBT + 4,6-DMDBT at 300 °C and 4.0 MPa. No DH-DMDBT was detected in our study. MoP/MCM-41(SR) showed a lower CO chemisorption capacity, a measure of the amount of active sites for metal phosphides, than MoP/MCM-41(R). This is probably due to the involvement of sulfur species in the MoP structure. In the HDS of DBT, about 1% TH-DBT was obtained, and BP yields were comparable for both catalysts. More CHB and BCH were produced on MoP/MCM-41(SR) than on MoP/MCM-41(R), indicating the higher HYD activity of MoP/MCM-41(SR). The TOF of MoP/MCM-41(SR) was nearly two times that of MoP/MCM-41(R), and the enhancement of the HDS activity was mainly due to the acceleration of HYD pathway. In the HDS of 4,6-DMDBT, the TOF of MoP/MCM-41(SR) was more than two times that of MoP/MCM-41(R). The yields of DMBP were low for both catalysts, and those of TH-DMDBT were comparable. For MoP/MCM-41(R), a small amount of HH-DMDBT was detected, in addition to TH-DMDBT, in the sulfur-containing hydrogenated intermediates. DMBCH, the fully hydrogenated hydrocarbon product, was dominant in the HDS products on MoP/MCM-41(SR) (63.2%), indicating the extremely high HYD activity of MoP/MCM-41(SR). In the simultaneous HDS of DBT and 4,6-DMDBT, the TOF of MoP/MCM-41(SR) was nearly two times that of MoP/MCM-41(R), and the product yields of DBT and 4,6-DMDBT were similar to those in independent HDS.

4. Discussion

4.1. MoP synthesis

The synthesis of MoP from oxidic precursors by temperature-programed reduction involves two solid reactants (MoO_3 and PO_x) and one gaseous (H_2) reactant.

$$MoO_3(s) + PO_x(s) + (x+3)H_2(g) \rightarrow MoP(s) + (x+3)H_2O(g) \quad (3)$$

It is generally accepted that the first step of the transformation is the reduction of MoO_3 to form MoO_2 in H_2 at relatively low temperature, as indicated by the TPR profiles of the MoP oxidic precursor (Fig. 4). The absence of diffraction peaks of MoO_3 and MoO_2 in Fig. 2a and b is probably due to the enhanced dispersion of Mo

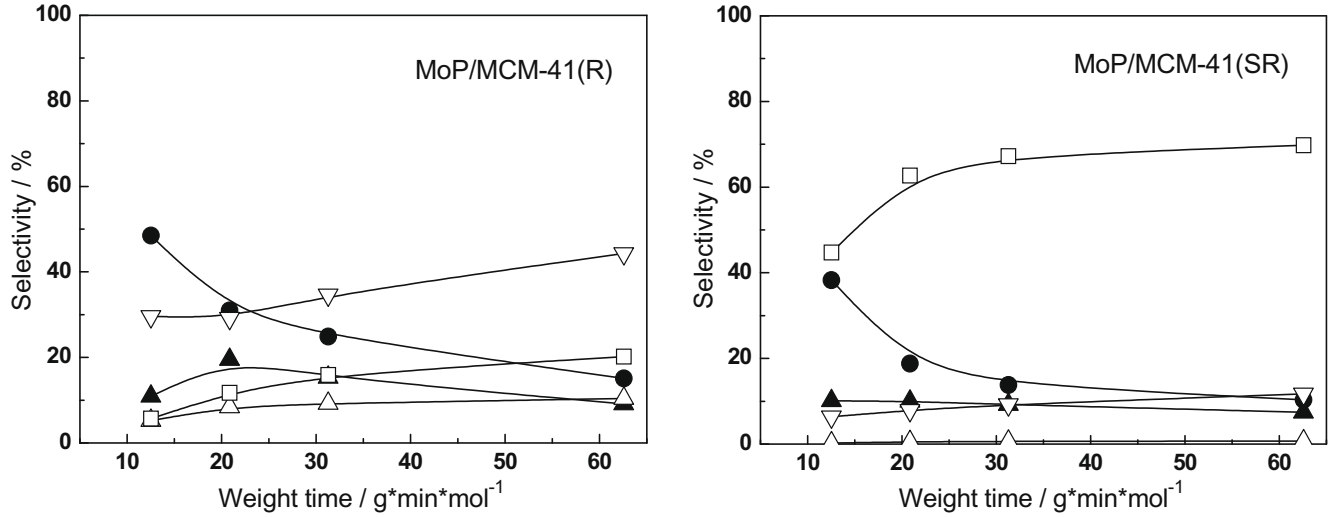

Fig. 13. Product selectivities in 4,6-DMDBT HDS over MoP/MCM-41(R) and MoP/MCM-41(SR): (●) TH-DMDBT, (▲) HH-DMDBT, (△) DMBP, (▽) DMCHB, (□) DMBCH.

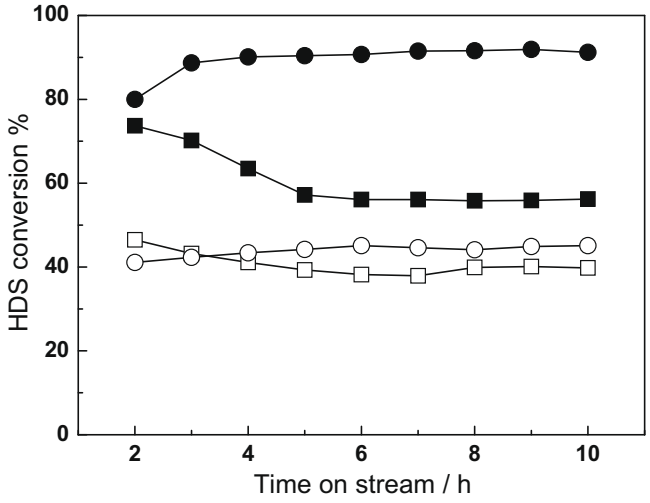

Fig. 14. Conversions of DBT and 4,6-DMDBT in simultaneous HDS over MoP/MCM-41(R) (open) and MoP/MCM-41(SR) (solid) at 300 °C and 4.0 MPa: (■,□) DBT, (●,○) 4,6-DMDBT.

oxides by phosphorous oxides [32]. At higher temperatures, phosphorous oxides are reduced to yield volatile phosphorous species, such as PH_3 or P, which migrates on the solid surface to react with the resulting MoO_2, leading to the formation of MoP.

MoO_3 can be converted to MoS_2 at 400 °C in H_2S/H_2 flow, whereas phosphorous oxides remain intact. At high temperature in the presence of H_2, MoS_2 and volatile phosphorous species will react to form MoP.

$$MoS_2(s) + PO_x(s) + (x+2)H_2(g) \rightarrow MoP(s) + xH_2O(g) + 2H_2S(g) \quad (4)$$

No H_2 consumption around 480 °C was observed in the TPR profile of the sulfided MoP precursor (Fig. 4c), suggesting that the sulfidation had turned Mo^{6+} to Mo^{4+} in the form of MoS_2. The subsequent high temperature reduction, i.e. the formation of MoP, was similar to that of the oxidic precursor.

The elemental analyses of the fresh MoP/MCM-41(SR) by XRF and XPS showed that sulfur was present both in the bulk and on the surface of MoP particles. The atomic ratio of (P + S/2)/Mo was close to unity, suggesting that each Mo atom might bind either to one P atom or to two S atoms. Moreover, the S/Mo ratio measured by XRF was identical to that measured by XPS, implying that sulfur was homogeneously distributed in MoP/MCM-41(SR). The only question left is whether there exists separate MoS_2 phase in MoP/MCM-41(SR).

Comparison of the HDS performance of MoP/MCM-41(SR) with that of mixtures of MoP/MCM-41(R) and MoS_2/MCM-41 revealed that MoP/MCM-41(SR) did not behave like a mixture of MoP/MCM-41(R) and MoS_2/MCM-41. In addition, the S 2p binding energy (162.4 eV) in the XPS spectrum of MoP/MCM-41(SR) was between those of S^{2-} species (161.7 eV) and S_2^{2-} (162.8–163.1 eV). It is therefore suggested that the active phase on MoP/MCM-41(SR) might not be a mixture of MoS_2 and MoP. No distinct difference was observed in the P 2p binding energy for MoP/MCM-41(SR) and MoP/MCM-41(R). On the other hand, the Mo 3d binding energy of MoP/MCM-41(SR) was slightly higher than that of MoP/MCM-41(R), probably due to the bonding between Mo and S. All these results suggest that S may be incorporated in the MoP structure.

HRTEM observations and XRD measurement revealed that the particle size of bulk MoP prepared by sulfidation–reduction was smaller than that by conventional temperature-programed reduction (Figs. 3a and b, and 2). Moreover, a careful comparison of the lattice spacing between the two samples indicated that bulk MoP crystal prepared by sulfidation–reduction possessed a slightly larger spacing (Fig. 3c and d). XRD patterns indicate that the framework of MoP structure prepared by sulfidation–reduction was similar (Figs. 1 and 2). The inclusion of sulfur atom in the structure of MoP may be responsible for the slight increase of lattice spacing in the crystals. XPS results show a shift of the Mo $3d_{5/2}$ binding energy from 228.6 to 229.1 eV, which is probably caused by the transfer of a small part of electron density from Mo to S, indicating that the incorporation of sulfur into the MoP structure decreases the electron density of Mo atom.

Recently, we reported the use of H_2S/H_2 to passivate Ni_2P/MCM-41, and found that sulfur might bind to the surface of Ni_2P in the passivation [33]. The H_2S-passivated Ni_2P crystal showed a smooth passivation layer whereas the conventional O_2-passivated one had a rough layer. A comparison of the images of MoP crystals prepared by different procedures (Fig. 3c and d) reveals that the inclusion of sulfur in MoP structure was favorable to protect the surface structure.

4.2. HDS performance

Among the metal phosphide hydrotreating catalysts, the HDS activity follows the order: MoP < WP < Ni_2P [6]. In the present study, MoP/MCM-41 (R) showed lower catalytic activity in the HDS of DBT (0.0079 s^{-1}) (Table 2) than Ni_2P/MCM-41 (0.012 s^{-1}) [33] at 300 °C and 4.0 MPa, but MoP/MCM-41(SR) exhibited a higher HDS activity (0.0153 s^{-1}). In the HDS of 4,6-DMDBT, the TOF of MoP/MCM-41 (R) was identical to that in the HDS of DBT, but the TOF of MoP/MCM-41(SR) was further improved. The activity improvement in the HDS of 4,6-DMDBT was accompanied by a significantly increased yield of DMBCH.

DMBCH is the fully hydrogenated non-sulfur HDS product of 4,6-DMDBT. Li et al. studied the kinetics of 4,6-DMDBT and its hydrogenated intermediates (TH-DMDBT, HH-DMDBT, and DH-DMDBT) over MoS_2/γ-Al_2O_3 [34]. The first step of 4,6-DMDBT involves two parallel reactions, i.e. the reaction of DMDBT to DMBP and that to TH-DMDBT. They found that the reaction rate of 4,6-DMDBT to TH-DMDBT was dramatically higher (34 times on MoS_2/γ-Al_2O_3) than that to DMBP in the presence of H_2S (10 kPa). In the present study, the yield of DMBP was very low on both MoP/MCM-41(R) and MoP/MCM-41(SR), indicating that the contribution of DDS pathway to the global HDS was negligible. The very low DDS activity is believed to arise from the steric hindrance when 4,6-DMDBT molecule is adsorbing in the σ-configuration (perpendicular to the surface) [35]. Similar to metal sulfides, the HDS of 4,6-DMDBT on supported MoP proceeds mainly through the HYD pathway. Li et al. [34] reported that the transformation of TH-DMDBT to HH-DMDBT was 20 times faster than that of HH-DMDBT to DH-DMDBT (0.04 mol $(g\,min)^{-1}$) in the subsequent HYD reaction steps over MoS_2/γ-Al_2O_3. On the other hand, the rate constant of the desulfurization of DH-DMDBT to DMBCH (1.35 mol $(g\,min)^{-1}$) was much larger than that of TH-DMDBT to DMCHB (0.10 mol $(g\,min)^{-1}$) and that of HH-DMDBT to DMCHB (0.07 mol $(g\,min)^{-1}$). In other words, the transformation of HH-DMDBT to DH-DMDBT is a "bottle neck" step, an acceleration of which will significantly increase the total desulfurization rate. In the HDS of 4,6-DMDBT on MoP/MCM-41(R), a small amount of HH-DMDBT was detected, and the predominant HDS product was DMCHB. It is suggested that the reaction of HH-DMDBT to DH-DMDBT might be slow on MoP/MCM-41(R), similar to the case of MoS_2/γ-Al_2O_3. In contrast, the predominant HDS product was DMBCH, and no DH-DMDBT was detected on MoP/MCM-41(SR).

According to the dependence of product selectivities on weight time in the HDS of 4,6-DMDBT (Fig. 13), it is not likely that DMBCH

Table 2
Catalytic performance of MoP/MCM-41 catalysts prepared via different procedures in the HDS of DBT and 4,6-DMDBT at 300 °C and 4.0 MPa.

Catalyst	CO uptake ($\mu mol\ g^{-1}$)	DBT conversion (%)	DMDBT conversion (%)	TOF (s^{-1})	Product yield (%)[a]								
					TH-DBT	BP	CHB	BCH	TH-DMDBT	HH-DMDBT	DMBP	DMCHB	DMBCH
HDS of DBT													
MoP/MCM-41(R)	16.3	39.5	–	0.0079	1.0	19.9	16.0	4.3	–	–	–	–	–
MoP/MCM-41(SR)	13.3	62.7	–	0.0153	1.1	18.0	28.1	11.2	–	–	–	–	–
HDS of DMDBT													
MoP/MCM-41(R)	16.3	–	45.9	0.0079	–	–	–	–	5.5	2.3	2.3	28.5	5.2
MoP/MCM-41(SR)	13.3	–	89.7	0.0189	–	–	–	–	5.9	0	2.8	17.7	63.2
HDS of DBT and DMDBT													
MoP/MCM-41(R)	16.3	39.8	45.1	0.0079	1.5	18.3	16.4	3.9	2.5	1.3	1.5	23.8	5.6
MoP/MCM-41(SR)	13.3	56.2	91.2	0.0165	1.1	16.5	24.3	8.6	2.5	0	2.3	20.1	63.8

[a] The feed concentrations were 0.8 wt% DBT, 0.8 wt% 4,6-DMDBT, and 0.4 wt% DBT plus 0.4 wt% 4,6-DMDBT.

arises from the hydrogenation of DMCHB. On the other hand, the enhancement of DMBCH production was accompanied by a significant decrease in TH-DMDBT with increasing weight time. It is therefore proposed that the transformation of HH-DMDBT to DH-DMDBT might be considerably accelerated, leading to the highest yield of DMBCH in the HDS product and the enhanced HDS activity. The HDS of 4,6-DMDBT on MoP/MCM-41(SR) may proceed predominantly through the route of DMDBT to TH-DMDBT to HH-DMDBT to DH-DMDBT to DMBCH. The transformation of TH-DMDBT to DMCHB competes with the above-mentioned route to some extent, leading to the second highest yield of DMCHB in the HDS product.

In the independent HDS of DBT and 4,6-DMDBT, the TOF of MoP/MCM-41(SR) was about two times that of MoP/MCM-41(R) (Table 2). Moreover, 4,6-DMDBT showed a substantially higher HDS activity than DBT. Because DBT and 4,6-DMDBT are present simultaneously in a real diesel fuel, it is important to know the HDS activity of the most refractory 4,6-DMDBT in the presence of DBT. The results of simultaneous HDS of DBT and 4,6-DMDBT indicated that the activity of 4,6-DMDBT was indeed higher than that of DBT over both MoP/MCM-41(R) and MoP/MCM-41(SR). The possible reason may be that the methyl groups have an electron-donating effect, thus DMDBT is more basic than DBT and hydrogenation should be easier. No comparison of HDS activity of DBT and 4,6-DMDBT over MoP has been reported. The higher activity of 4,6-DMDBT might be related with the synergy of the stronger adsorption of 4,6-DMDBT [31] and the high hydrogenation activity of MoP.

The incorporation of sulfur species might give rise to slight distortion or modification of the MoP crystal surface. The surface change and the decreased particle size of MoP, which correspond to a high dispersion, might favor the π adsorption of HH-DMDBT, accelerating the hydrogenation of HH-DMDBT to DH-DMDBT.

Many research groups reported the enhancements of HDS activity of metal phosphides with the involvement of sulfur. According to the characterization results of fresh and spent metal phosphide catalysts, Oyama et al. proposed that metal phosphosulfides might be the active sites in HDS [11,12]. Sawhill et al. found that an O_2-passivated Ni_2P/SiO_2 catalyst showed a higher HDS activity when it was subjected to sulfidation by H_2S/H_2 than to H_2 reduction [15]. Wu et al. also reported an enhancement of HDS activity of sulfided MoP/SiO_2 in the HDS of thiophene, but high temperature presulfidation led to a decrease in HDS activity [36]. They attributed the decreased activity to the formation of irreversibly bonded sulfur species at high temperature sulfidation, because only the reversibly bonded sulfur species contributed to the HDS activity. In our recent work [33], we found that the HDS activity of Ni_2P/MCM-41 was well correlated with the sulfur content of the spent catalyst. In all these studies, sulfur was introduced after metal phosphides had been synthesized, and the sulfur species were supposed to be present on the surface or subsurface of the metal phosphides.

Loboué et al. prepared unsupported nickel phosphides by the reduction of $NiPS_3$ [37]. The obtained nickel phosphides, Ni_5P_4 and Ni_2P, exhibited a much higher HDS activities than MoS_2 in the HDS of thiophene. The elemental analysis revealed the presence of sulfur in the spent catalysts, but they did not compare the HDS activity with Ni_2P prepared by the conventional temperature-programed reduction method. So it is impossible to determine whether the sulfur species, which was introduced prior to the synthesis of Ni_2P, had a positive effect on the HDS performance of Ni_2P/SiO_2. Korányi reported that H_2S facilitated the reduction process to form Ni_2P and Co_2P, leading to enhanced activities in thiophene HDS [38].

MoP/MCM-41(R) and MoP/MCM-41(SR) did not show a distinct difference in the XRD patterns, indicating that the crystal structures were the same in both catalysts (Fig. 1). However, a dramatic difference in catalytic activity was observed in the HDS of DBT and 4,6-DMDBT. The significantly enhanced HDS activity may be attributed mainly to the incorporation of sulfur into the bulk and surface of the MoP crystals. The incorporation may lead to the formation of more active sites, such as phosphosulfide structure, on the surface. Moreover, the inclusion of sulfur in bulk structure of MoP may lead to a slight distortion of MoP framework structure, as evidence by XRD measurement, HRTEM observation, and XPS analysis.

5. Conclusions

Our results demonstrate that a sulfidation step in the temperature-programed reduction improved dramatically the HDS performance of the resulting MoP/MCM-41(SR). Moreover, the sulfidation step gave rise to a lowered threshold reduction temperature in the preparation of MoP/MCM-41. The comparison of HDS performance of MoP/MCM-41(SR) with the mixtures of MoP/MCM-41 and MoS_2/MCM-41 excludes the synergy of separate MoS_2 and MoP phases in MoP/MCM-41(SR). The Mo $3d_{5/2}$ binding energy of MoP/MCM-41(SR) was slightly higher than that of MoP/MCM-41(R), which is probably caused by the transfer of a small part of electron density from Mo to S. The TOFs of MoP/MCM-41(SR) were about two times those of MoP/MCM-41(R) in the HDS of DBT, the HDS of 4,6-DMDBT, and the simultaneous HDS of DBT and 4,6-DMDBT. The enhancement of HDS activity of MoP/MCM-41(SR) was accompanied by an accelerated HYD activity. 4,6-DMDBT exhibited much higher activity than DBT in the simultaneous HDS over MoP/MCM-41(SR) whereas slightly higher over MoP/MCM-41(R). The HDS of 4,6-DMDBT on MoP/MCM-41(SR)

proceeded predominantly through the route of DMDBT to TH-DMDBT to HH-DMDBT to DH-DMDBT to DMBCH, whereas on MoP/MCM-41(R) through the route of DMDBT to TH-DMDBT to DMCHB. The differences in performance and predominant route may arise mainly from the structural modification by sulfur species, which dramatically accelerated the reaction of HH-DMDBT to DH-DMDBT. XRD characterization and HRTEM observation indicated that the inclusion of sulfur in the bulk structure of MoP lead to a slight increase of lattice spacing in the crystals.

Acknowledgments

The authors acknowledge financial support from the Natural Science Foundation of China (20333030, 20503003, and 20773020), the NCET, and the 111 Project. The authors thank Prof. R. Prins (ETH) for his helpful discussion.

Appendix A. Supplementary material

Supplementary data associated with this article can be found, in the online version, at doi:10.1016/j.jcat.2009.07.003.

References

[1] S. Li, J.S. Lee, J. Catal. 178 (1998) 119.
[2] M. Nagai, A. Irisawa, S. Omi, J. Phys. Chem. B 102 (1998) 7619.
[3] C. Stinner, R. Prins, Th. Weber, J. Catal. 191 (2000) 438.
[4] D.C. Phillips, S.J. Sawhill, R. Self, M.E. Bussell, J. Catal. 207 (2002) 266.
[5] S.T. Oyama, J. Catal. 216 (2003) 343.
[6] W.R.A.M. Robinson, J.N.M. van Gestel, T.I. Korányi, S. Eijsbouts, A.M. van der Kraan, J.A.R. van Veen, V.H.J. de Beer, J. Catal. 161 (1996) 539.
[7] S. Yang, C. Liang, R. Prins, J. Catal. 237 (2006) 118.
[8] S. Yang, R. Prins, Chem. Commun. (2005) 4178.
[9] L. Song, W. Li, G. Wang, M. Zhang, K. Tao, Catal. Today 125 (2007) 137.
[10] Y. Shu, S.T. Oyama, Carbon 43 (2005) 1517.
[11] S.T. Oyama, X. Wang, Y.-K. Lee, K. Bando, F.G. Requejo, J. Catal. 210 (2002) 207.
[12] S.T. Oyama, X. Wang, Y.-K. Lee, W.-J. Chun, J. Catal. 221 (2004) 263.
[13] C. Stinner, R. Prins, Th. Weber, J. Catal. 202 (2001) 187.
[14] V. Zuzaniuk, R. Prins, J. Catal. 219 (2003) 85.
[15] S.J. Sawhill, D.C. Phillips, M.E. Bussell, J. Catal. 215 (2003) 208.
[16] F. Sun, W. Wu, Z. Wu, J. Guo, Z. Wei, Y. Yang, Z. Jiang, F. Tian, C. Li, J. Catal. 228 (2004) 298.
[17] A. Wang, T. Kabe, Chem. Commun. (1999) 2067.
[18] A. Wang, L. Ruan, Y. Teng, X. Li, M. Lu, J. Ren, Y. Wang, Y. Hu, J. Catal. 229 (2005) 314.
[19] W. Qian, A. Ishihara, S. Ogawa, T. Kabe, J. Phys. Chem. 98 (1994) 907.
[20] I.I. Abu, K.J. Smith, J. Catal. 241 (2006) 356.
[21] R. Thomas, E.M. van Oers, V.H.J. de Beer, J. Medema, J.A. Moulijn, J. Catal. 76 (1982) 241.
[22] P. Clark, X. Wang, S.T. Oyama, J. Catal. 207 (2002) 256.
[23] D.J. Sajkowski, J.T. Miller, G.W. Zajac, T.I. Morrison, H. Chen, D.R. Fazzini, Appl. Catal. 62 (1990) 205.
[24] D.S. Zingg, L.E. Makovsky, R.E. Tischer, F.R. Brown, D.M. Hercules, J. Phys. Chem. 84 (1980) 2898.
[25] P.A. Spevack, N.S. McIntyre, J. Phys. Chem. 97 (1993) 11020.
[26] Y. Okamoto, K. Fukino, T. Imanaka, S.J. Teranishi, J. Catal. 74 (1982) 173.
[27] Th. Weber, J.C. Muijsers, J.W. Niemantsverdriet, J. Phys. Chem. 99 (1995) 9194.
[28] Th. Weber, J.C. Muijsers, J.H.M.C. van Wolput, C.P.J. Verhagen, J.W. Niemantsverdriet, J. Phys. Chem. 100 (1996) 14144.
[29] P.A. Spevack, N.S. McIntyre, J. Phys. Chem. 97 (1993) 11031.
[30] R. Shafi, G.J. Hutchings, Catal. Today 59 (2000) 423.
[31] T. Kabe, A. Ishihara, Q. Zhang, Appl. Catal. A 97 (1993) L1.
[32] P. Atanasova, T. Halachev, J. Uchytil, M. Kraus, Appl. Catal. 38 (1988) 235.
[33] X. Duan, Y. Teng, A. Wang, V.M. Kogan, X. Li, Y. Wang, J. Catal. 261 (2009) 232.
[34] X. Li, A. Wang, M. Egorova, R. Prins, J. Catal. 250 (2007) 283.
[35] T. Kabe, A. Ishihara, W. Qian, Hydrodesulfurization and Hydrodenitrogenation, Kodansha, Wiley-VCH, Weinheim, Tokyo, 1999. p. 53.
[36] Z. Wu, F. Sun, W. Wu, Z. Feng, C. Liang, Z. Wei, C. Li, J. Catal. 222 (2004) 41.
[37] H. Loboué, C. Guillot-Deudon, A.F. Popa, A. Lafond, B. Rebours, C. Pichon, T. Cseri, G. Berhault, C. Geantet, Catal. Today 130 (2008) 63.
[38] T.I. Korányi, Appl. Catal. A 239 (2003) 253.